

# Harnessing Bounded-Support Evolution Strategies for Policy Refinement

Ethan Hirschowitz

The University of Sydney, Australia  
*ehir9923@uni.sydney.edu.au*

Fabio Ramos

The University of Sydney, Australia  
 NVIDIA, USA  
*fabio.ramos@sydney.edu.au*

## Abstract

Improving competent robot policies with on-policy RL is often hampered by noisy, low-signal gradients. We revisit Evolution Strategies (ES) as a policy-gradient proxy and localize exploration with bounded, antithetic triangular perturbations, suitable for policy refinement. We propose Triangular-Distribution ES (TD-ES) which pairs bounded triangular noise with a centered-rank finite-difference estimator to deliver stable, parallelizable, gradient-free updates. In a two-stage pipeline — PPO pretraining followed by TD-ES refinement — this preserves early sample efficiency while enabling robust late-stage gains. Across a suite of robotic manipulation tasks, TD-ES raises success rates by 26.5% relative to PPO and greatly reduces variance, offering a simple, compute-light path to reliable refinement.

## 1 Introduction

Reinforcement learning (RL) equips robots with the ability to acquire complex behaviors directly from interaction, sidestepping laborious analytic modeling and expensive data collection processes [Ibarz *et al.*, 2021; Mirchandani *et al.*, 2024]. While gradient-based deep RL has achieved impressive results in dexterous manipulation, legged locomotion and autonomous driving domains [OpenAI *et al.*, 2018; Tang *et al.*, 2024; Wang *et al.*, 2023], its practical deployment remains a challenge [Henderson *et al.*, 2017; Dulac-Arnold *et al.*, 2019; Fu *et al.*, 2020; Engstrom *et al.*, 2020].

Crucially, popular policy-gradient methods such as PPO [Schulman *et al.*, 2017] approximate gradients from stochastic rollouts using surrogate objectives and clipping. In a refinement context, when near competent policies, these estimates become small-magnitude, high-variance and sensitive to hyperparameters, making fine-grained refinement unreliable and costly [Engstrom *et al.*, 2020; Wołczyk *et al.*, 2024; Kirkpatrick

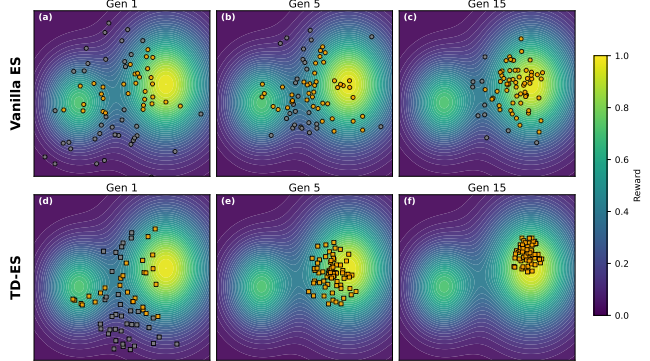


Figure 1: Parameter space exploration comparison between Gaussian ES and TD-ES across generations. Both methods search from a PPO checkpoint toward higher-reward regions. Gaussian ES (top row) uses unbounded perturbations that spread widely, while TD-ES (bottom row) employs bounded triangular perturbations for localized exploration. Orange points indicate candidates in high-reward regions, grey points in lower-reward areas. TD-ES achieves more focused exploration with higher sample efficiency in beneficial regions.

*et al.*, 2017]. Yet in robotics applications, even modest performance gains can yield considerable practical value [Dulac-Arnold *et al.*, 2019].

Evolution Strategies (ES) [Beyer and Schwefel, 2002; Wierstra *et al.*, 2014; Salimans *et al.*, 2017] show promise for policy refinement due to their gradient-free nature and robustness to local optima, making them well-suited to refining competent policies where gradient-based methods may struggle with small, noisy signals. However, standard ES with unconstrained (e.g. Gaussian) perturbations is poorly matched to refinement: much of the sampling mass lies far from the current parameters, inflating estimator variance and reducing refinement efficiency [Wong *et al.*, 2024; Majid *et al.*, 2021; Pagliuca *et al.*, 2019].

We propose a two-stage refinement pipeline that cou-

ples the data efficiency of gradient methods with the stability and parallelism of a gradient-free search. Stage 1 uses PPO to obtain a competent policy and coarse ascent directions. Stage 2 introduces *Triangular-Distribution Evolution Strategies* (TD-ES): an ES variant that samples parameter-space perturbations from a bounded-support triangular distribution, concentrating probability near zero while enforcing a hard radius on updates. This implements a soft trust region in parameter space, reducing estimator variance, mitigating catastrophic regressions, and focusing exploration where the objective is locally smooth, as illustrated in Figure 1. **Specifically, we make the following contributions:**

1. We formulate TD-ES, a localized ES refinement method using antithetic, unit-variance triangular perturbations and a centered-rank finite-difference estimator, yielding a simple, compute-light gradient proxy constructed from scalar returns only.
2. We provide a principled view of TD-ES as estimating the gradient of a smoothed objective and show (under standard smoothness) second-order accuracy in the smoothing scale; we explain how bounded support induces trust-region-like behavior without requiring backpropagation or KL constraints.
3. We specify a practical two-stage schedule (PPO pre-training  $\rightarrow$  TD-ES refinement) with equal interaction budgets.
4. We demonstrate our approach improves PPO on a variety of robotic manipulation tasks, and demonstrate through ablation that this improvement is enhanced through our bounded-support approach.

## 2 Related Work

Our approach builds on several complementary research directions in reinforcement learning and evolutionary optimization. We review trust-region methods for policy optimization, gradient-evolution hybrid approaches, distribution design for ES, and recent work on triangular distributions in an RL context.

### Trust-Region Policy Optimization

Trust-region methods such as TRPO [Schulman *et al.*, 2015] and PPO [Schulman *et al.*, 2017] localize updates by constraining the policy’s change (via KL penalties or clipping), a design that has proven dependable in locomotion and manipulation [Heess *et al.*, 2017; Kuo *et al.*, 2023]. Importantly, these algorithms approximate gradients from stochastic rollouts; near competent policies the signals become small-magnitude and high-variance, and performance can hinge on sensitive hyperparameters [Engstrom *et al.*, 2020; Wołczyk *et al.*, 2024; Kirkpatrick *et al.*, 2017]. Trust-region ideas have also

been adapted to ES (e.g., TRES [Liu *et al.*, 2019]), typically by constraining action space divergences between successive policies. In contrast, our approach enforces parameter space locality during population generation by sampling from a bounded-support distribution, yielding a simple, compute-light mechanism that curbs destabilizing updates without backpropagation.

### Gradient–Evolution Hybrids

A growing line of work mixes gradient-based updates with evolutionary search. Examples include joint-update schemes such as CEM-RL [Pourchot and Sigaud, 2018] and PPO–ES mixtures [Sigaud, 2022], as well as interleaved variants (e.g., EPO [Mustafaoglu *et al.*, 2025]). While these hybrids can improve performance, meta-analyses note added scheduling complexity and potential drift [Lin *et al.*, 2024; Bai *et al.*, 2023]. We adopt a simpler sequential hand-off tailored to refinement: PPO is used first to enter a high-reward basin, after which a localized, gradient-free ES performs constrained search within that basin. This avoids running two optimizers concurrently while retaining the complementary strengths of each.

### Distribution Design for ES

ES is attractive for massive parallelism and robustness to sparse rewards [Salimans *et al.*, 2017; Such *et al.*, 2017; Ha and Schmidhuber, 2018; Conti *et al.*, 2017; Huizinga and Clune, 2018], yet its sample efficiency in high-dimensional policies suffers when isotropic Gaussian perturbations disperse candidates far from the incumbent potentially reducing sample efficiency [Majid *et al.*, 2021; Wong *et al.*, 2024; Pagliuca *et al.*, 2019]. CMA-ES can improve locality via learned covariance [Hansen, 2016; Uchida *et al.*, 2024], but its  $O(d^2)$  cost limits applicability with deep networks [Nishida *et al.*, 2018]. An orthogonal approach is to shape the perturbation law itself to bias exploration toward local moves; we follow this direction using bounded-support perturbations (see “Triangular Distributions For Reinforcement Learning” below and Section 4).

### Triangular Distributions For Reinforcement Learning

Petersen *et al.* [Petersen and Ermon, 2024] explored triangular distributions in RL and provided an implementation we use. We differ by employing the triangular law for parameter space ES in a refinement setting, emphasizing bounded support to localize exploration and stabilize updates (see Section 4).

## 3 Preliminaries

### 3.1 Problem Setting and Notation

We consider an episodic Markov decision process (MDP) with state space  $\mathcal{S}$ , action space  $\mathcal{A}$ , horizon  $H$ ,

and stochastic dynamics  $p(s_{t+1} \mid s_t, a_t)$ . At each time step the agent receives a scalar reward  $r_t = r(s_t, a_t)$ . Under a policy  $\pi_\theta(a \mid s)$ , parameterized by  $\theta \in \mathbb{R}^d$ , an episode generates a trajectory  $\tau = (s_0, a_0, r_0, \dots, s_{H-1}, a_{H-1}, r_{H-1})$  according to  $\pi_\theta$  and  $p$ .

We maximize the expected discounted return:

$$J(\theta) = \mathbb{E}_{\tau \sim \pi_\theta} \left[ \sum_{t=0}^{H-1} \gamma^t r_t \right], \quad \gamma \in (0, 1] \quad (1)$$

Unless stated otherwise we use the diagonal-Gaussian policy

$$\pi_\theta(a \mid s) = \mathcal{N}(a; \mu_\theta(s), \text{diag } \sigma_\pi^2(s)), \quad (2)$$

where the network outputs the mean  $\mu_\theta(s)$  and log-standard deviation  $\log \sigma_\pi(s)$ . We distinguish two noise scales:  $\sigma_\pi$  governs on-policy exploration in *action space*, while a separate scale  $\sigma_{\text{ES}}$  will control *parameter space* perturbations in the evolutionary refinement stage.

### 3.2 Evolution Strategies Recap

In classic ES, at step  $t$ , a population of  $n$  perturbed parameter vectors is drawn from an isotropic Gaussian centered at the current point  $\theta_t$ ,

$$\theta_t^{(i)} = \theta_t + \sigma_{\text{ES}} \delta_t^{(i)}, \quad \delta_t^{(i)} \sim \mathcal{N}(0, I), \quad (3)$$

where the superscript  $(i)$  denotes the  $i^{\text{th}}$  individual in the current population.

Each  $\theta_i$  instantiates a candidate policy  $\pi_{\theta_i}$ . After parallel rollouts we form the Monte Carlo score-function (likelihood-ratio) gradient estimator [Salimans *et al.*, 2017] and update the center as in (4).

$$g_t = \frac{1}{n\sigma_{\text{ES}}} \sum_{i=1}^n J(\theta_i) \delta_i, \quad \theta_{t+1} = \theta_t + \alpha_t g_t. \quad (4)$$

This formulation communicates only scalar returns, making ES trivially parallelizable.

The gradient-free nature of ES, combined with its robustness to local optima [Salimans *et al.*, 2017] and embarrassingly parallel structure, makes it particularly well-suited for policy refinement scenarios where gradient-based methods may encounter diminishing returns near competent policies.

However, isotropic noise explores the entire parameter space, which can be inefficient when the policy is already near a good solution. We make the connection between (4) and a policy-gradient proxy precise in the following section.

### 3.3 ES as a Policy-Gradient Proxy

Classical policy-gradient methods estimate  $\nabla_\theta J(\theta)$  for the objective in (1) by injecting randomness in *action*

*space* under the policy (2). ES provides an alternative in *parameter space*: sample perturbations  $\delta$  as in (3), evaluate returns  $J(\theta + \sigma_{\text{ES}}\delta)$  for the same objective (1), and aggregate them into the Monte Carlo estimator (4). Formally, define the Gaussian-smoothed objective

$$J_\sigma(\theta) = \mathbb{E}_{\delta \sim \mathcal{N}(0, I)} [J(\theta + \sigma_{\text{ES}}\delta)]. \quad (5)$$

The gradient of  $J_\sigma(\theta)$  is

$$\nabla_\theta J_\sigma(\theta) = \frac{1}{\sigma_{\text{ES}}} \mathbb{E}_{\delta \sim \mathcal{N}(0, I)} [J(\theta + \sigma_{\text{ES}}\delta) \delta]. \quad (6)$$

Consequently, the Monte-Carlo average  $g_t$  in (4) is an unbiased estimator of the exact gradient in (6), yet it needs only scalar returns.

In other words, ES performs policy gradient by approximating  $\nabla_\theta J$  with  $\nabla_\theta J_\sigma$ . Under mild smoothness ( $J \in C^2$ ), a second-order Taylor expansion gives  $\nabla_\theta J_\sigma(\theta) = \nabla_\theta J(\theta) + \mathcal{O}(\sigma_{\text{ES}}^2)$ ; thus smaller  $\sigma_{\text{ES}}$  lowers smoothing bias but raises Monte Carlo variance, mitigated by larger populations, antithetic pairs, and a constant baseline.

Because the estimator uses sampled perturbations, their *distribution and scale* determine variance and the locality of search; in refinement, unconstrained isotropic exploration is often wasteful. As discussed in Section 2, on-policy methods such as PPO also approximate gradients from rollouts but become small-magnitude and high-variance near competent policies. Consequently, choosing the perturbation distribution is crucial for efficient late-stage improvement; in Section 4 we instantiate this with a bounded-support sampler that concentrates exploration near  $\theta$  and stabilizes refinement.

### 3.4 Triangular Distribution

We consider the symmetric triangular distribution with mode at zero and support  $[-a, a]$ , whose probability density function is

$$f(x) = \begin{cases} \frac{1}{a} \left(1 - \frac{|x|}{a}\right), & \text{if } |x| \leq a, \\ 0, & \text{otherwise.} \end{cases} \quad (7)$$

Here  $a > 0$  is the *half-width* (the distance from the mode to either boundary). For this distribution, the mean is 0 and the variance is  $\text{Var}(X) = a^2/6$ .

In our implementation, we set the half-width  $a = \sigma_{\text{ES}}$ . This yields perturbations  $\varepsilon$  with support  $[-\sigma_{\text{ES}}, \sigma_{\text{ES}}]$  and can be sampled as  $\varepsilon = \sigma_{\text{ES}}(U - V)$  where  $U, V \sim \text{Uniform}(0, 1)$  and are independent. This parameterization directly controls the maximum parameter exploration, and enables a natural comparison between the bounded-support triangular distribution and unbounded Gaussian perturbations at the same scale parameter.

Figure 2 shows the theoretical triangular PDF with support  $[\mu - a, \mu + a]$  (here  $\mu = 0$ ) with the half-width  $a$

indicated. We overlay this with a subset of our samples from an experiment to verify that the sampler matches the theoretical distribution.

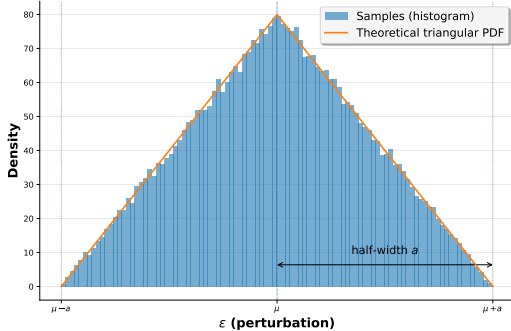


Figure 2: Theoretical triangular distribution PDF overlaid with a subset of our actual samples (histogram).

## 4 Methodology

### 4.1 Problem Formulation

We operate in a policy refinement context, where the initial anchor policy  $\pi_{\theta_0}$ , parameterized by a neural network, is obtained through training with PPO [Schulman *et al.*, 2017], chosen for its empirical reliability on robotic tasks [Mittal *et al.*, 2023; Heess *et al.*, 2017; Kuo *et al.*, 2023; Rupam Mahmood *et al.*, 2018].

This anchor policy is safe and reasonably successful, but not yet optimal. Our objective is to find a refined parameter vector  $\theta^*$  where

$$\theta^* = \arg \max_{\theta} J(\theta). \quad (8)$$

Although we consider a policy refinement context when presenting our methods, the full benefits of our work can be harnessed by invoking a 2-stage sequential training framework. This is discussed further in Section 4.6.

### 4.2 Bounded-Support Perturbations for ES

We refine the PPO anchor  $\theta_0$  using Evolution Strategies. At iteration  $t$  we maintain a center  $\theta_t$  (initialized as  $\theta_0$ ) and replace the isotropic Gaussian sampler (3) with a bounded-support, zero-mean, factorized base distribution  $q$  to localize search and improve refinement efficiency.

Concretely, we use the symmetric triangular law on each coordinate with support  $[-\sigma_{\text{ES}}, \sigma_{\text{ES}}]$  and mode 0 (detailed in 3.4),

$$q_{\Delta}(\varepsilon_k) = \begin{cases} \frac{1}{\sigma_{\text{ES}}} \left(1 - \frac{|\varepsilon_k|}{\sigma_{\text{ES}}}\right), & \text{if } |\varepsilon_k| \leq \sigma_{\text{ES}}, \\ 0, & \text{otherwise,} \end{cases} \quad (9)$$

$$q(\varepsilon) = \prod_{k=1}^d q_{\Delta}(\varepsilon_k).$$

Given  $\varepsilon_i \sim q$  we construct  $n = 2m$  candidates via antithetic pairs

$$\theta_i^{\pm} = \theta_t \pm \sigma_{\text{ES}} \varepsilon_i, \quad i = 1, \dots, m. \quad (10)$$

The bounded support implies  $\|\theta_i^{\pm} - \theta_t\|_{\infty} \leq \sigma_{\text{ES}}$  while the mode at zero concentrates probability on small perturbations and further reduces estimator variance by concentrating sampling probability on perturbations near the current parameters, where the objective function is more likely to exhibit locally smooth behavior. Figure 3 empirically demonstrates this effect, showing that triangular perturbations achieve 83.1% average variance reduction compared to Gaussian perturbations during refinement.

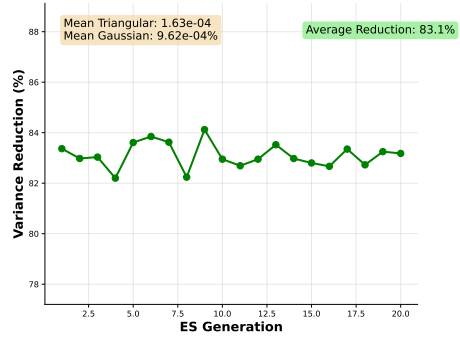


Figure 3: Relative reduction in gradient estimator variance achieved by triangular perturbations compared to Gaussian perturbations during ES refinement. The y-axis shows the percentage by which triangular ES reduces variance relative to Gaussian ES at each generation, computed from multiple independent gradient estimates. Positive values indicate lower variance for triangular perturbations. The bounded support of triangular distributions consistently reduces estimator variance throughout the refinement process, demonstrating the stabilizing effect of localized parameter-space exploration.

### 4.3 Gradient Approximation under Bounded-Support ES

Given antithetic pairs  $\{\theta_i^{\pm}\}_{i=1}^m$  from (10), let  $J_i^{\pm} = J(\theta_i^{\pm})$  be their scalar returns and set  $n = 2m$ . We compute centered ranks within the generation by ranking the  $n$  returns from worst to best, mapping ranks to  $[-\frac{1}{2}, \frac{1}{2}]$ , and standardizing to unit variance; denote the resulting scores by  $\tilde{J}_i^{\pm}$ . Our update forms a finite-difference search direction using these scores:

$$g_t = \frac{1}{m \sigma_{\text{ES}}} \sum_{i=1}^m (\tilde{J}_i^+ - \tilde{J}_i^-) \varepsilon_i, \quad (11)$$

$$\theta_{t+1} = \theta_t + \alpha_t g_t.$$

Antithetic pairing cancels even-order terms in the finite difference and reduces variance. With standardized, zero-mean perturbations ( $\mathbb{E}[\varepsilon] = 0$ ,  $\mathbb{E}[\varepsilon\varepsilon^\top] = I$ ) and smooth  $J$ , (11) is a *constant-scaled central-difference proxy*: when raw returns are used its expectation is

$$\mathbb{E}[g_t] = c \nabla_\theta J(\theta_t) + \mathcal{O}(\sigma_{\text{ES}}^2), \quad (12)$$

for some constant  $c > 0$ . In our implementation with a prefactor  $1/(m\sigma_{\text{ES}})$  we have  $c = 2$ , while the normalized two-sided estimator  $\frac{1}{2m\sigma_{\text{ES}}} \sum_{i=1}^m (J_i^+ - J_i^-) \varepsilon_i$  gives  $c = 1$ . With centered ranks as our default, the estimator is scale- and shift-invariant, remains directionally aligned in the small- $\sigma_{\text{ES}}$  regime, and exhibits the same  $\mathcal{O}(\sigma_{\text{ES}}^2)$  truncation order; the effective constant depends on the score transform and local return distribution and is absorbed into  $\alpha_t$ .

#### 4.4 Trust-Region-Like Locality from Bounded Support

The sampler in (10) induces trust-region-like behavior directly in parameter space. First, bounded support guarantees a hard per-parameter radius (proportional to  $\sigma_{\text{ES}}$ ), capping the maximum excursion of any coordinate in a generation. Second, the triangular mode at zero concentrates probability on small perturbations, increasing the frequency of locally linear samples and reducing estimator variance. Empirically, these two effects (i) mitigate catastrophic regressions during refinement, (ii) improve the stability of late-stage updates without additional backpropagation or KL constraints, and (iii) preserve ES’s embarrassingly parallel rollout structure.

#### 4.5 Triangular-Distribution Evolution Strategies (TD-ES)

We now summarize the full procedure as Triangular-Distribution Evolution Strategies (TD-ES) which combines the bounded-support sampler (10) with the centered-rank estimator (11).

*Rollout notation.* As in Sec. 3,  $s_t$  is the state at time  $t$ ,  $a_t$  is the sampled action,  $r_t$  is the reward,  $H$  is the horizon, and  $\gamma$  is the RL discount;  $\mu_\theta(\cdot)$  is the policy mean and  $\sigma_a$  is the fixed action std used during ES (see 5.2). ROLLOUT returns one Monte Carlo sample of Eq. (1).

#### 4.6 Two-Stage PPO and TD-ES Schedule

We adopt a sequential hand-off approach: PPO for initial skill acquisition, followed by TD-ES for stable refinement. Rather than using fixed budget allocations, we empirically determine the handoff point based on when PPO achieves a competent policy — typically identified when learning curves show diminishing returns or when success rates reach a reasonable baseline (e.g., 40-60% task completion). This ensures TD-ES begins refinement from a meaningful anchor point rather than from random

---

#### Algorithm 1: TD-ES

---

```

Input : anchor policy parameters  $\theta_0$ , pairs  $m$ ,  

       iterations  $T$ , perturb. scale  $\sigma_{\text{ES}}$ , step size  $\alpha$ ,  

       action std  $\sigma_a$ , decays  $\lambda_\sigma$   

Output: Refined parameters  $\theta$ 
1  $\theta \leftarrow \theta_0$ 
2 for  $t = 1$  to  $T$  do
3   for  $i = 1$  to  $m$  do
4     sample  $\varepsilon_i \sim q_\Delta$  // triangular noise on  $[-\sigma_{\text{ES}}, \sigma_{\text{ES}}]$ 
5      $\theta_i^\pm \leftarrow \theta \pm \sigma_{\text{ES}} \varepsilon_i$  // antithetic candidates
6      $J_i^\pm \leftarrow \text{ROLLOUT}(\theta_i^\pm; \sigma_a)$  // scalar episodic returns
7     form centered ranks  $\tilde{J}_i^\pm$  over  $\{J_j^\pm\}$  // unit variance
8      $g \leftarrow \frac{1}{m\sigma_{\text{ES}}} \sum_{i=1}^m (\tilde{J}_i^+ - \tilde{J}_i^-) \varepsilon_i$  // cf. Eq. (11)
9      $\theta \leftarrow \theta + \alpha g$  // parameter update
10     $\sigma_{\text{ES}} \leftarrow \lambda_\sigma \sigma_{\text{ES}}$ 
11 return  $\theta$ 
12 Function Rollout( $\theta; \sigma_a$ )
13   run one episode with  $a_t \sim \mathcal{N}(\mu_\theta(s_t), \sigma_a^2 I)$ 
14   return  $\sum_{t=0}^{H-1} \gamma^t r_t$  //  $\gamma$  is the RL discount (not a decay)

```

---

initialization. The total interaction budget remains fixed across all compared methods to ensure fair evaluation.

## 5 Experimental Setup

Our experiments are designed to evaluate whether refinement with our bounded-support approach is able to benefit performance across a variety of robotic manipulation tasks. We also aim to identify how robust these benefits are across conditions. All experiments were run on a single NVIDIA RTX 4070 using Isaac Lab [Mittal *et al.*, 2023] as the GPU-accelerated physics simulator for robotic manipulation, via its vectorized environment interface for parallel rollouts. For statistical robustness, we repeat every configuration with nine independent random seeds and reuse the same seed set across all methods. Fairness across methods is ensured as methods share identical observation/action spaces and identical total environment step budgets; specific budget allocations are detailed in Section 5.2.

We report success rates rather than cumulative reward because binary task completion is more interpretable and directly relevant to real-world deployment than engineered reward signals. Following best practices for reliable RL evaluation [Agarwal *et al.*, 2021], aggregate performance is summarized with the Interquartile Mean (IQM) and 95% stratified bootstrap confidence intervals, which yields robust estimates with fewer runs and reduces sensitivity to outliers. We additionally report the probability of improvement  $P(\text{TD-ES} \rightarrow \text{PPO})$  using the Mann-Whitney U statistic to quantify the likelihood that our method outperforms the baseline. For individual task analysis, per-task results are presented as mean  $\pm$  standard deviation.

Section 5.1 outlines the tasks/environments used for evaluation, and Section 5.2 lists specific implementation details to support reproducibility. Section 6 then proceeds in three parts: (i) Aggregate Performance versus existing baseline to establish gains, (ii) a Per-Task Analysis to localize where improvements concentrate, and (iii) a Performance Distribution Analysis to examine robustness across difficulty factors and tail behavior (5th/95th percentiles).

## 5.1 Task Domains

We evaluate our approach on three robotic manipulation tasks using a 7-DoF Franka Panda arm, chosen to test policy refinement across different precision requirements. Lift-Cube and Open-Drawer use 8D joint-space control (7 joints + gripper), while Peg-Insert employs 6D task-space control with constrained roll/pitch for tool alignment. Figure 4 provides visual overview and technical specifications.

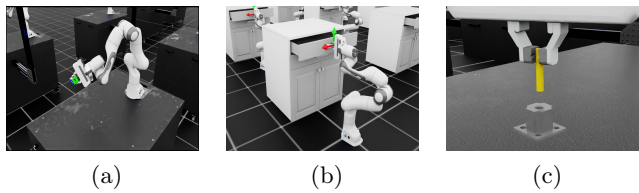


Figure 4: Robotic manipulation tasks: (a) Lift-Cube with 36D observations and 4096 environments, (b) Open-Drawer with 31D observations and 4096 environments, (c) Peg-Insert with 19D observations and 512 environments due to contact modeling demands.

**Lift-Cube** requires grasping and positioning a cube within 4cm of a target. Refinement challenges include achieving spatial precision while maintaining grasp stability, where small parameter improvements reduce tolerance violations and grip failures.

**Open-Drawer** involves grasping a handle and opening a drawer at least 30cm while maintaining handle contact. Success depends on reliable initial grasping, coordinated pulling motion, and sufficient extension distance — all areas where fine-grained parameter adjustments provide significant benefits.

**Peg-Insert** demands inserting an 8mm peg into an 8mm hole (0.114mm clearance) with sub-millimeter positioning accuracy. Success requires the peg within 2.5mm laterally and 1mm above target depth. This contact-rich task exemplifies high-precision manipulation where minor control improvements dramatically impact insertion success by reducing jamming and misalignment.

## 5.2 Implementation Details

We use task-specific budgets with PPO→TD-ES splits based on learning dynamics: Lift-Cube (12,000 steps,

83:17 split), Open-Drawer (19,200 steps, 67:33), Peg-Insert (4,470 steps, 67:33). PPO uses standard hyperparameters ( $\gamma = 0.99$ ,  $\lambda = 0.95$ ,  $\epsilon = 0.2$ ) with task-specific learning rates and network architectures. TD-ES initializes from PPO checkpoints with  $\sigma_a = 0.01$ , decay  $\lambda_\sigma = 0.99$ , and floor  $\sigma_{\min} = 1 \times 10^{-3}$ . Key hyperparameters are shown in Table 1.

Table 1: Key task-specific hyperparameters.

Parameter	Lift-Cube	Open-Drawer	Peg-Insert
PPO learning rate	$1 \times 10^{-4}$	$5 \times 10^{-4}$	$1 \times 10^{-3}$
PPO Episodes per update	24	96	24
TD-ES $\sigma_{\text{ES}}$	0.0125	0.025	0.03
TD-ES learning rate	0.005	0.01	0.01

We compare our method against PPO-only (full budget without refinement) and Gaussian ES (identical to TD-ES but with unbounded Gaussian perturbations), isolating the bounded-support contribution.

## 6 Results

### 6.1 Aggregate Performance

Table 2 presents aggregate task success rates across all methods. Our results demonstrate that ES-based refinement provides consistent improvements over PPO alone, with TD-ES offering additional systematic benefits.

The results show a clear progression in refinement effectiveness. TD-ES achieves an IQM success rate of 85.0%, compared to Gaussian ES's 73.7% and PPO's 67.2%. This demonstrates systematic improvements through ES-based refinement, with our bounded-support approach providing additional gains beyond standard Gaussian perturbations. The Mann-Whitney U test indicates 73.7% probability that TD-ES outperforms PPO. We also found that there was a **69.2% probability that TD-ES outperforms Gaussian ES**, demonstrating statistically significant improvement across the method progression.

### 6.2 Per-Task Analysis

Table 3 reveals how refinement benefits scale with task requirements.

The results demonstrate systematic improvements through the refinement progression. Open-Drawer shows the most dramatic benefits from bounded-support refinement, with TD-ES achieving near-perfect success (97.8%) while drastically reducing variance ( $\sigma$ : 31.4%  $\rightarrow$  1.9%). On the Peg-Insert task our approach shows a substantial 18.5 percentage point improvement over the PPO baseline, with a much tighter clustering. Lift-Cube shows a consistent 5.4 percentage point improvement with reduced variance.

Table 2: Aggregate success rate across all tasks using robust statistical measures.

Method	IQM (95% CI)	Mean (95% CI)	P(Improvement vs PPO)
PPO	67.2% (55.8–77.5%)	65.3% (56.0–74.6%)	–
PPO→Gaussian ES	73.7% (62.4–83.3%)	69.9% (60.6–79.1%)	55.6% (39.6–70.7)%
PPO→TD-ES	<b>85.0% (77.7–91.9%)</b>	<b>83.6% (78.2–88.9%)</b>	<b>73.7% (59.4–86.9%)</b>

Table 3: Per-task success rates (mean  $\pm$  std) across experimental runs.

Task	PPO	PPO→Gaussian ES	PPO→TD-ES
Lift-Cube	$75.2\% \pm 18.8\%$	$76.0\% \pm 19.6\%$	$80.6\% \pm 15.2\%$
Open-Drawer	$67.0\% \pm 31.4\%$	$75.8\% \pm 33.2\%$	$97.8\% \pm 1.9\%$
Peg-Insert	$53.8\% \pm 19.4\%$	$57.8\% \pm 15.1\%$	$72.3\% \pm 5.7\%$

The variance reduction pattern is particularly striking: TD-ES consistently achieves the lowest performance variability across all tasks, with the most pronounced stabilization occurring on precision-demanding tasks. This suggests that bounded-support perturbations effectively prevent destabilizing parameter excursions during refinement.

### 6.3 Bounded-Support Ablation

To isolate the bounded-support contribution, we directly compare PPO→TD-ES against PPO→Gaussian ES using identical refinement protocols. Both methods initialize from the same PPO checkpoints and use identical hyperparameters, with the only difference being triangular versus Gaussian perturbation distributions.

The comparison reveals systematic advantages of bounded-support perturbations. At the aggregate level, TD-ES achieves 85.0% IQM success compared to Gaussian ES’s 73.7%, representing a 15% relative improvement in refinement effectiveness. A Mann-Whitney U test indicated 73.7% probability that TD-ES outperforms PPO compared to 55.6% for Gaussian ES, demonstrating stronger statistical evidence for TD-ES improvements. Further, another Mann-Whitney U test indicated that there is a 69.2% chance that TD-ES actually outperforms Gaussian ES, further highlighting the benefits of the bounded-support approach.

The per-task analysis reveals task-dependent benefits of bounded-support perturbations. For Lift-Cube, both methods provide similar modest improvements over PPO, with TD-ES achieving slightly higher success (80.6% vs 76.0%) and reduced variance (15.2% vs 19.6%). Open-Drawer shows the most dramatic bounded-support advantage: while Gaussian ES provides moderate improvement (67.0%  $\rightarrow$  75.8%), TD-ES achieves near-perfect performance (97.8%) with drastically reduced variance (1.9% vs 33.2%). Peg-Insert demonstrates consistent bounded-support benefits, with TD-ES substantially outperforming Gaussian ES (72.3% vs 57.8%) while maintaining much tighter performance

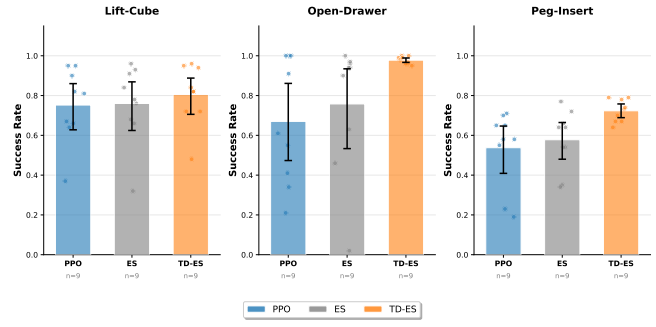


Figure 5: Individual run success rates. Our approach shows reduced variance across all tasks, with particularly tight clustering on precision-demanding tasks (Open-Drawer, Peg-Insert).

clustering.

The variance reduction pattern is particularly revealing: TD-ES consistently achieves lower performance variability than Gaussian ES across all tasks, with the effect being most pronounced on precision-demanding tasks. This suggests that bounded-support perturbations provide enhanced stability during refinement by preventing parameter excursions that degrade performance in high-precision scenarios.

Importantly, hyperparameters were tuned for triangular distributions and may not be optimal for Gaussian perturbations. However, this controlled comparison demonstrates that bounded-support perturbations systematically enhance ES refinement effectiveness beyond what standard Gaussian perturbations can achieve, providing strong evidence for our bounded-support hypothesis in policy refinement contexts.

### 6.4 Performance Distribution Analysis

Figure 5 shows the distribution of individual run performance across each task.

The individual run distributions clearly illustrate the systematic benefits of our bounded-support refinement approach. The three-method comparison shows consis-

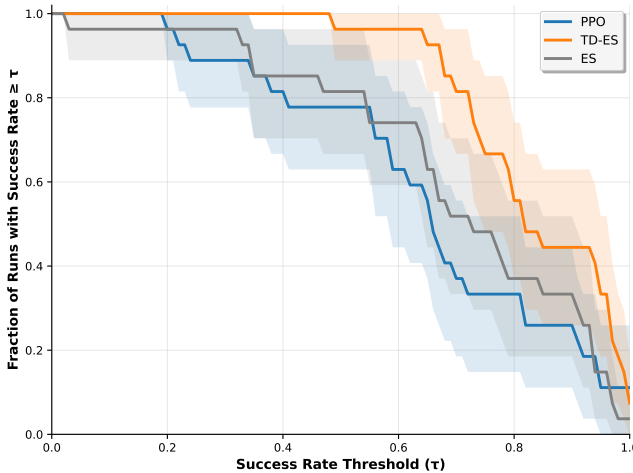


Figure 6: Performance profiles showing fraction of runs achieving success rates above threshold  $\tau$ . TD-ES curve dominates PPO across all thresholds, indicating more reliable high-performance outcomes.

tent ranking: PPO provides the baseline, Gaussian ES offers moderate improvements with increased variance in some cases, and TD-ES delivers the strongest performance with reduced variability.

As recommended by Agarwal et al. [2021], we plot performance profiles in Figure 6 to demonstrate the cumulative distribution of success rates across all experimental runs.

This performance profile demonstrates that our approach is superior across all success rate thresholds. The TD-ES curve remains consistently above PPO, with particularly pronounced advantages in the high-performance region ( $\tau > 0.7$ ). At a 80% success threshold, TD-ES achieves this performance in approximately 50% of runs compared to PPO’s 20%, highlighting the practical reliability improvements for deployment scenarios where consistent task completion is critical.

## 7 Conclusion and Future Work

We have presented Triangular-Distribution Evolution Strategies (TD-ES), a bounded-support approach for policy refinement that addresses gradient-based limitations in late-stage training. Our two-stage PPO→TD-ES framework demonstrates systematic improvements over both PPO alone and standard Gaussian ES across robotic manipulation tasks, with particularly pronounced benefits on precision-demanding scenarios.

The key insight is that bounded-support perturbations provide trust-region-like behavior in parameter space without backpropagation or KL constraints. By concentrating exploration near competent policies while preventing destabilizing excursions, TD-ES achieves im-

proved performance and enhanced reliability. Results show clear progression: PPO establishes baselines, Gaussian ES provides moderate benefits, and TD-ES delivers substantial improvements with reduced variance.

Several limitations are deserve mention. Refinement effectiveness remains constrained by anchor policy quality, with performance varying across seeds. Computational constraints limited evaluation to moderate-complexity tasks, leaving scaling to more demanding scenarios an open question.

Future work offers promising directions. Stronger pre-training methods may reduce seed sensitivity and establish higher-quality anchors. Alternative bounded-support distributions — including Beta, Kumaraswamy, trapezoidal, raised-cosine, and truncated Gaussian forms — may better capture actuator constraints and provide smoother gradient approximations. Finally, extending evaluation to complex manipulation suites would strengthen understanding of when these methods excel.

The systematic improvements demonstrated suggest that bounded-support perturbations offer a principled, practical approach to policy refinement with broader potential in robotics and beyond.

## References

- [Agarwal et al., 2021] Rishabh Agarwal, Max Schwarzer, Pablo Samuel Castro, Aaron Courville, and Marc G Bellemare. Deep reinforcement learning at the edge of the statistical precipice. *arXiv [cs.LG]*, August 2021.
- [Bai et al., 2023] Hui Bai, Ran Cheng, and Yaochu Jin. Evolutionary reinforcement learning: A survey. *arXiv [cs.NE]*, March 2023.
- [Beyer and Schwefel, 2002] Hans-Georg Beyer and Hans-Paul Schwefel. Evolution strategies - a comprehensive introduction. *Natural Computing*, 1:3–52, 03 2002.
- [Conti et al., 2017] Edoardo Conti, Vashisht Madhavan, Felipe Petroski Such, Joel Lehman, Kenneth O Stanley, and Jeff Clune. Improving exploration in evolution strategies for deep reinforcement learning via a population of novelty-seeking agents. *arXiv [cs.AI]*, December 2017.
- [Dulac-Arnold et al., 2019] Gabriel Dulac-Arnold, Daniel Mankowitz, and Todd Hester. Challenges of real-world reinforcement learning. *arXiv [cs.LG]*, April 2019.
- [Engstrom et al., 2020] Logan Engstrom, Andrew Ilyas, Shibani Santurkar, Dimitris Tsipras, Firdaus Janoos, Larry Rudolph, and Aleksander Madry. Implementation matters in deep policy gradients: A case study on PPO and TRPO. *arXiv [cs.LG]*, May 2020.

[Fu *et al.*, 2020] Justin Fu, Aviral Kumar, Ofir Nachum, George Tucker, and Sergey Levine. D4RL: Datasets for deep data-driven reinforcement learning. *arXiv [cs.LG]*, April 2020.

[Ha and Schmidhuber, 2018] David Ha and Jürgen Schmidhuber. World models. *arXiv [cs.LG]*, March 2018.

[Hansen, 2016] Nikolaus Hansen. The CMA evolution strategy: A tutorial. *arXiv [cs.LG]*, April 2016.

[Heess *et al.*, 2017] Nicolas Heess, Dhruva Tb, Srinivasan Sriram, Jay Lemmon, Josh Merel, Greg Wayne, Yuval Tassa, Tom Erez, Ziyu Wang, S M Ali Eslami, Martin Riedmiller, and David Silver. Emergence of locomotion behaviours in rich environments. *arXiv [cs.AI]*, July 2017.

[Henderson *et al.*, 2017] Peter Henderson, Riashat Islam, Philip Bachman, Joelle Pineau, Doina Precup, and David Meger. Deep reinforcement learning that matters. *arXiv [cs.LG]*, September 2017.

[Huizinga and Clune, 2018] Joost Huizinga and Jeff Clune. Evolving multimodal robot behavior via many stepping stones with the combinatorial multi-objective evolutionary algorithm. *arXiv [cs.NE]*, July 2018.

[Ibarz *et al.*, 2021] Julian Ibarz, Jie Tan, Chelsea Finn, Mrinal Kalakrishnan, Peter Pastor, and Sergey Levine. How to train your robot with deep reinforcement learning; lessons we've learned. *arXiv [cs.RO]*, February 2021.

[Kirkpatrick *et al.*, 2017] James Kirkpatrick, Razvan Pascanu, Neil Rabinowitz, Joel Veness, Guillaume Desjardins, Andrei A Rusu, Kieran Milan, John Quan, Tiago Ramalho, Agnieszka Grabska-Barwinska, Demis Hassabis, Claudia Clopath, Dharshan Kumaran, and Raia Hadsell. Overcoming catastrophic forgetting in neural networks. *Proc. Natl. Acad. Sci. U. S. A.*, 114(13):3521–3526, March 2017.

[Kuo *et al.*, 2023] Ping-Huan Kuo, Wei-Cyuan Yang, Po-Wei Hsu, and Kuan-Lin Chen. Intelligent proximal-policy-optimization-based decision-making system for humanoid robots. *Advanced Engineering Informatics*, 56:102009, 2023.

[Lin *et al.*, 2024] Yuanguo Lin, Fan Lin, Guorong Cai, Hong Chen, Lixin Zou, and Pengcheng Wu. Evolutionary reinforcement learning: A systematic review and future directions. *arXiv [cs.NE]*, February 2024.

[Liu *et al.*, 2019] Guoqing Liu, Li Zhao, Feidiao Yang, Jiang Bian, Tao Qin, Nenghai Yu, and Tie-Yan Liu. Trust region evolution strategies. In *Proceedings of the Thirty-Third AAAI Conference on Artificial Intelligence and Thirty-First Innovative Applications of Artificial Intelligence Conference and Ninth AAAI Symposium on Educational Advances in Artificial Intelligence*, AAAI'19/IAAI'19/EAAI'19, Honolulu, Hawaii, USA, 2019. AAAI Press.

[Majid *et al.*, 2021] Amjad Yousef Majid, Serge Saaybi, Tomas van Rietbergen, Vincent Francois-Lavet, R Venkatesha Prasad, and Chris Verhoeven. Deep reinforcement learning versus evolution strategies: A comparative survey. *arXiv [cs.LG]*, September 2021.

[Mirchandani *et al.*, 2024] Suvir Mirchandani, Suneel Belkhale, Joey Hejna, Evelyn Choi, Md Sazzad Islam, and Dorsa Sadigh. So you think you can scale up autonomous robot data collection? *arXiv [cs.RO]*, November 2024.

[Mittal *et al.*, 2023] Mayank Mittal, Calvin Yu, Qinx Yu, Jingzhou Liu, Nikita Rudin, David Hoeller, Jia Lin Yuan, Ritvik Singh, Yunrong Guo, Hammad Mazhar, Ajay Mandlekar, Buck Babich, Gavriel State, Marco Hutter, and Animesh Garg. Orbit: A unified simulation framework for interactive robot learning environments. *arXiv [cs.RO]*, January 2023.

[Mustafaoglu *et al.*, 2025] Zelal Su “lain Mustafaoglu, Keshav Pingali, and Risto Miikkulainen. Evolutionary policy optimization. *arXiv [cs.LG]*, April 2025.

[Nishida *et al.*, 2018] Kouhei Nishida, Hernan Aguirre, Shota Saito, Shinichi Shirakawa, and Youhei Akimoto. Parameterless stochastic natural gradient method for discrete optimization and its application to hyperparameter optimization for neural network. *arXiv [cs.LG]*, September 2018.

[OpenAI *et al.*, 2018] OpenAI, Marcin Andrychowicz, Bowen Baker, Maciek Chociej, Rafal Jozefowicz, Bob McGrew, Jakub Pachocki, Arthur Petron, Matthias Plappert, Glenn Powell, Alex Ray, Jonas Schneider, Szymon Sidor, Josh Tobin, Peter Welinder, Lilian Weng, and Wojciech Zaremba. Learning dexterous in-hand manipulation. *arXiv [cs.LG]*, August 2018.

[Pagliuca *et al.*, 2019] Paolo Pagliuca, Nicola Milano, and Stefano Nolfi. Efficacy of modern neuro-evolutionary strategies for continuous control optimization. *arXiv [cs.NE]*, December 2019.

[Petersen and Ermon, 2024] Felix Petersen and Stefano Ermon. Triangular distributions for reinforcement learning. In *Conference on Robot Learning (CoRL) 2024 Workshop on Differentiable Simulation for Robot Learning*, October 2024.

[Pourchot and Sigaud, 2018] Aloïs Pourchot and Olivier Sigaud. CEM-RL: Combining evolutionary and gradient-based methods for policy search. *arXiv [cs.LG]*, October 2018.

[Rupam Mahmood *et al.*, 2018] A Rupam Mahmood, Korenkevych Dmytro, Vasan Gautham, Ma William,

and Bergstra James. Benchmarking reinforcement learning algorithms on real-world robots. *arXiv [cs.LG]*, September 2018.

[Salimans *et al.*, 2017] Tim Salimans, Jonathan Ho, Xi Chen, Szymon Sidor, and Ilya Sutskever. Evolution strategies as a scalable alternative to reinforcement learning. *arXiv [stat.ML]*, March 2017.

[Schulman *et al.*, 2015] John Schulman, Sergey Levine, Philipp Moritz, Michael I Jordan, and Pieter Abbeel. Trust region policy optimization. *arXiv [cs.LG]*, February 2015.

[Schulman *et al.*, 2017] John Schulman, Filip Wolski, Prafulla Dhariwal, Alec Radford, and Oleg Klimov. Proximal policy optimization algorithms. *arXiv [cs.LG]*, July 2017.

[Sigaud, 2022] Olivier Sigaud. Combining evolution and deep reinforcement learning for policy search: A survey. *arXiv [cs.LG]*, March 2022.

[Such *et al.*, 2017] Felipe Petroski Such, Vashisht Madhavan, Edoardo Conti, Joel Lehman, Kenneth O Stanley, and Jeff Clune. Deep neuroevolution: Genetic algorithms are a competitive alternative for training deep neural networks for reinforcement learning. *arXiv [cs.NE]*, December 2017.

[Tang *et al.*, 2024] Chen Tang, Ben AbbateMatteo, Jiaheng Hu, Rohan Chandra, Roberto Martín-Martín, and Peter Stone. Deep reinforcement learning for robotics: A survey of real-world successes. *arXiv [cs.RO]*, August 2024.

[Uchida *et al.*, 2024] Kento Uchida, Ryoki Hamano, Masahiro Nomura, Shota Saito, and Shinichi Shirakawa. CMA-ES for safe optimization. *arXiv [cs.NE]*, May 2024.

[Wang *et al.*, 2023] Letian Wang, Jie Liu, Hao Shao, Wenshuo Wang, Ruobing Chen, Yu Liu, and Steven L Waslander. Efficient reinforcement learning for autonomous driving with parameterized skills and priors. *arXiv [cs.RO]*, May 2023.

[Wierstra *et al.*, 2014] Daan Wierstra, Tom Schaul, Tobias Glasmachers, Yi Sun, Jan Peters, and Jürgen Schmidhuber. Natural evolution strategies. *Journal of Machine Learning Research*, 15(27):949–980, 2014.

[Wołczyk *et al.*, 2024] Maciej Wołczyk, Bartłomiej Cupiał, Mateusz Ostaszewski, Michał Bortkiewicz, Michał Zająć, Razvan Pascanu, Łukasz Kuciński, and Piotr Miłoś. Fine-tuning reinforcement learning models is secretly a forgetting mitigation problem. *arXiv [cs.LG]*, February 2024.

[Wong *et al.*, 2024] Annie Wong, Jacob de Nobel, Thomas Bäck, Aske Plaat, and Anna V Kononova. Solving deep reinforcement learning tasks with evolution strategies and linear policy networks. *arXiv [cs.LG]*, February 2024.